Resonance induced by a spatially periodic force in the reaction-diffusion system

Chenggui Yao,[1,2] Zhiwei He,[1,3] JinMing Luo,[4] and Jianwei Shuai[2,*]
[1]*Department of Mathematics, Shaoxing University, Shaoxing 312000, China*
[2]*Department of Physics, Xiamen University, Xiamen 361005, People's Republic of China*
[3]*Wuhan Institute of Physics and Mathematics, Chinese Academy of Sciences, Wuhan 430071, China*
[4]*College of Science, China University of Mining and Technology, Xuzhou 221000, China*
(Received 2 March 2015; revised manuscript received 11 April 2015; published 6 May 2015)

The stimulus-dynamic response is an important topic in physics. In this work, we study the dynamics in the reaction-diffusion system subjected to a weak signal and a spatially periodic force. We find that the response of the system to the weak signal is enhanced largely by the spatially periodic force, which is termed spatially periodic-force-induced resonance. In particular, the response becomes stronger when the spatial frequency is chosen such that the system synchronizes with spatially periodic force. This combinative behavior, i.e., the spatially periodic-force-induced resonance and the spatial-synchronization-enhanced resonance, is of great interest and may shed light on our understanding of the dynamics of nonlinear systems subjected to spatially periodic force in responding to a weak signal.

DOI: 10.1103/PhysRevE.91.052901 PACS number(s): 05.45.Xt

I. INTRODUCTION

Stochastic resonance, the phenomenon of the response of nonlinear systems to a weak periodic signal enhanced by an appropriate strength of noise, has drawn much attention in nonlinear science for more than 30 years [1–5]. This unusual, constructive role of noise on nonlinear systems has been studied extensively in physical, chemical, and biological systems [6–11]. Analogous to noise in stochastic resonance, the other driving sources have also been shown to be able to play a similar role. For example, the system's response to a weak low-frequency signal can become maximal with an optimal intensity of high-frequency periodic force. This phenomenon, called vibrational resonance, was first reported by Landa and Blekhman [12]. Tessone *et al.* found that the appropriate quenched noise could lead to a resonant effect in the globally coupled bistable and excitable systems responding to a weak periodic signal [13–15]. This phenomenon has been named diversity-induced resonance. Since then, many studies have been devoted to the unusual effect of quenched noise and high-frequency force in the framework of the resonance. Gassel *et al.* studied the interplay of additive and multiplicative diversity (the so-called doubly diversity-induced resonance [16]) and the diversity-sustained pattern formation in subexcitable media [17]. Chen *et al.* reported the structural-diversity-enhanced cellular ability to detect subthreshold extracellular signals in biological systems [18]. The study of vibrational resonance has also been widely investigated in various systems, including excitable [19–22], bistable [23–26], and spatially extended systems [27–31].

Recently, the effect of spatially periodic force on dynamic behaviors has been investigated in reaction-diffusion systems. Page *et al.* explored the effects of spatial force on pattern formation in the Gierer-Meinhardt reaction-diffusion model, and they found that the spatial force can both increase the range and complexity of possible patterns and enhance the robustness of pattern selection [32]. Dolnik *et al.* investigated the role of spatially periodic force on the hexagonal pattern of Turing structures in the chlorine dioxide-iodine-malonic acid reaction-diffusion system, and they showed many defects that break the symmetry of the pattern [33]. Manor *et al.* reported wave-number locking and pattern formation in a two-dimensional system driven by a one-dimensional periodic weak force [34].

We are curious about how the spatially periodic force influences the response of the reaction-diffusion system to the weak signal in this paper. In such a reaction-diffusion system subjected to a weak signal and spatially periodic force, we find the effect of optimal amplification of the weak signal. In other words, the spatially periodic force can induce resonant behavior with the increase of amplitude of the spatial force. More interestingly, the resonance can be largely enhanced when the system synchronizes with the spatially periodic force at some special frequencies.

II. MODEL

We focus on the following bistable reaction-diffusion system:

$$\partial_t X = X - X^3 + D\partial_x^2 X + A\cos(\omega t) + c\sin\left(2\pi f\frac{x}{L}\right), \tag{1}$$

where $X(x,t)$ $(0 \leqslant x \leqslant L)$ is the potential height at position x for time t. D is the strength of diffusion. The undiffused model describes the overdamped motion in the bistable potential $U(X) = \frac{X^4}{4} - \frac{X^2}{2}$ subjected to the weak periodic signal with the angular frequency ω and amplitude A. $c\sin(2\pi f\frac{x}{L})$ is a spatial force with the spatial frequency f. All our numerical results are obtained through the standard Euler approach of the reaction-diffusion equation [Eq. (1)] with periodic boundary conditions for the fixed time step $\Delta t = 0.01$ and grid distance $\Delta x = 0.1$.

To quantify the response of the system to the weak periodic signal, we define a temporal resonance factor Q_t that is

*Corresponding author: jianweishuai@xmu.edu.cn

given by

$$Q_t = \sqrt{Q_{t1}^2 + Q_{t2}^2},$$
$$Q_{t1} = \frac{1}{T}\int_{T_0}^{T_0+T} Y(t)\cos(\omega t)dt, \quad (2)$$
$$Q_{t2} = \frac{1}{T}\int_{T_0}^{T_0+T} Y(t)\sin(\omega t)dt.$$

The temporal resonance factor Q_t characterizes the signal output of the mean field $Y(t) = \frac{1}{L}\int_0^L X(x,t)dx$ at the input frequency ω. Both sufficiently large T_0 and T should be chosen; large T_0 is used for discarding the transient processing and large T for a proper measurement of average over time. The temporal resonance factor Q_t can provide a precise measure of the responding ability of the system to the weak periodic signal at frequency ω. To quantify the responding ability of the system to the spatially periodic force at spatial frequency f, we also define a spatial resonance factor Q_s,

$$Q_s = \sqrt{Q_{s1}^2 + Q_{s2}^2},$$
$$Q_{s1} = \frac{1}{L}\int_0^L Z(x)\cos 2\pi f\frac{x}{L}dx, \quad (3)$$
$$Q_{s2} = \frac{1}{L}\int_0^L Z(x)\sin 2\pi f\frac{x}{L}dx,$$

where $Z(x) = \frac{1}{T}\int_{T_0}^{T_0+T} X(x,t)dt$.

III. SPATIALLY PERIODIC-FORCE-INDUCED RESONANCE

Figures 1(a) and 1(b) show the spatial resonance factor Q_s as a function of f and c in a three-dimensional (3D) and a two-dimensional (2D) contour plot, respectively. Obviously, Q_s increases with the amplitude of spatial force for fixed frequency f, and nonmonotonically decreases with the frequency of spatial force for fixed amplitude c [Figs. 1(a) and 1(b)]. The temporal resonance factor Q_t versus f and

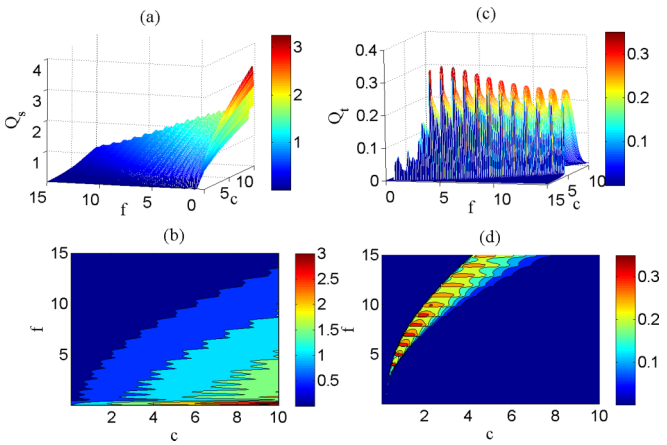

FIG. 1. (Color online) The 3D plot and contour of the amplification factor Q_t [(a) and (b)] and Q_s [(c) and (d)] as a function of f and c, respectively. The parameters $A = 0.2$, $\omega = \frac{2\pi}{T}$, $D = 0.1$, $L = 10$, and $T = 100$ are chosen.

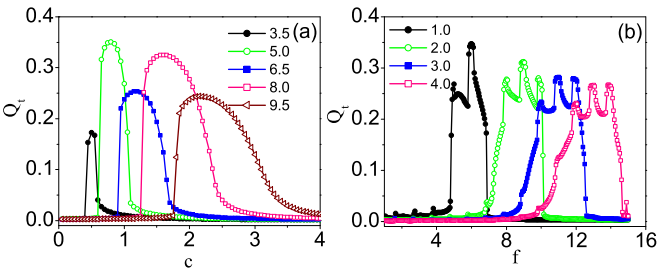

FIG. 2. (Color online) (a) Q_t against c and (b) against f. In (a) from left to right, $f = 3.5$, 5, 6.5, 8, and 9.5, respectively. In (b) from left to right, $c = 1$, 2, 3, and 4, respectively.

c in a 3D and a 2D contour plot is presented in Figs. 1(c) and 1(d), respectively. One can observe that the influence of spatially periodic force on the response of the system to the weak signal is remarkable. The temporal resonance factor Q_t becomes large at some region of c and f of the spatial force, which we term spatially periodic-force-induced resonance.

As some examples, Figs. 2(a) and 2(b) illustrate the temporal resonance factor Q_t against c for $f = 3.5$, 5, 6.5, 8, and 9.5, and against f for $c = 1$, 2, 3, and 4, respectively. From Fig. 2, the spatially periodic-force-induced resonance can be seen clearly in the c direction for a fixed f, and multiresonance emerges in the f direction for a fixed c. The peaks of the temporal resonance factor Q_t are obtained with spatial force at some specific amplitudes c and frequencies f, indicating that the resonance is enhanced by those special spatial forces.

We now analyze how the system responds to different diffusion coefficient D and modulation periods T of the weak signal. In Fig. 3(a), the dependence of Q_t on c for different D is exhibited. One can notice that the optimal $c_{\rm opt}$ increases with an increment of D, and the local maximum of temporal resonance factor Q_t depends on the diffusion coefficient D. The local maximum of temporal resonance factor Q_t against D is shown in Fig. 3(b). The local maximum Q_t nonmonotonously

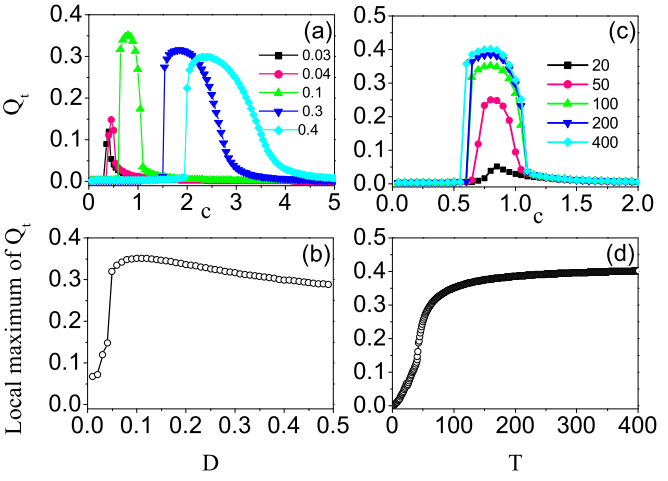

FIG. 3. (Color online) (a) Dependence of Q_t on c for different diffusion coefficients D, and (b) the local maximum value of Q_t as a function of D at $T = 100$. (c) Q_t against c for different periods of weak signal T, and (d) the local maximum value of Q_t against T at $D = 0.1$.

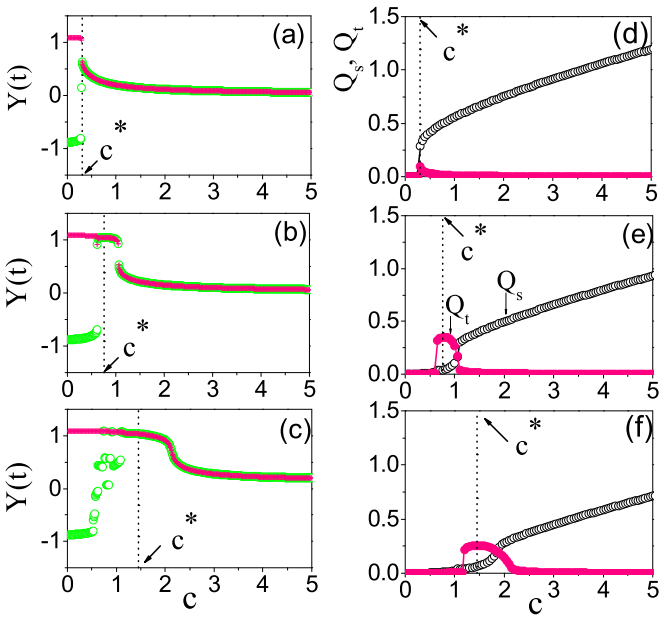

FIG. 4. (Color online) (a)–(c) Bifurcation diagrams of $Y(t) = \frac{1}{L}\int_0^L X(x,t)dx$ for the local maximal values with positive initial conditions (green solid points) and negative initial conditions (pink pluses) for different values of f: $f = 2.0$, 5.0, and 7.5, respectively, indicating the system transitions from a bistable to a monostable state across the peak position c^*. (d)–(f) The plots of Q_t and Q_s against c, $f = 2.0$, 5.0, and 7.5, respectively.

depends on the diffusion coefficient D. There exists an optimal diffusion coefficient such that the response of the system to the weak signal become maximal. The temporal resonance factor Q_t against c for a different period T of the weak signal is shown in Fig. 3(c), indicating that Q_t increases and quickly saturates as T increases (comparing these five curves). In Fig. 3(d), we plot the local maximum of temporal resonance factor Q_t as a function of the period T of the weak signal. It can be seen that for large T, the local maxima of temporal resonance reach a constant value.

The occurrence of vibrational, diversity-induced, and stochastic resonance indicates that the forcing sources can change the dynamics of populations, giving rise to a system transition from a bistable to a monostable state, and causing the amplitude to become maximal at the transition point. Therefore, the peak position for the resonant behavior should correspond to the system threshold from a bistable to a monostable state [13,31]. Our numerical result shows that this mechanism can be generalized to spatially periodic-force-induced resonance. Figures 4(a)–4(c) show bifurcation diagrams of mean field $Y(t) = \frac{1}{L}\int_0^L X(x,t)dx$ for different spatial frequencies f, where the transition from a bistable to a monostable state with increasing c across point c^* (c^* is the peak position) is clearly shown. Figures 4(d)–4(f) illustrate Q_t and Q_s against c, which shows $Q_t \gg Q_s$ for the moderate amplitude c, whereas $Q_t \ll Q_s$ if the amplitude increases [Figs. 4(e) and 4(f)]. These results reveal that the spatial force acts like a modulator and the oscillating frequency of the system switches from temporal frequency to spatial frequency with increasing amplitude. Based on these observations, Q_t monotonically increases with c for small c as the system transfers from a bistable to a monostable state. After that, Q_t monotonically decreases with c due to the change of oscillation mode. In the following, we show that the spatially periodic-force-induced resonance comes from not only the transition from a bistable to a monostable state [Figs. 4(a)–4(c)] but also the change of the oscillation mode [Figs. 4(d)–4(f)].

To show the detailed dynamics, the continuous spatiotemporal evolution of $X(x,t)$ is shown in Fig. 5 with positive

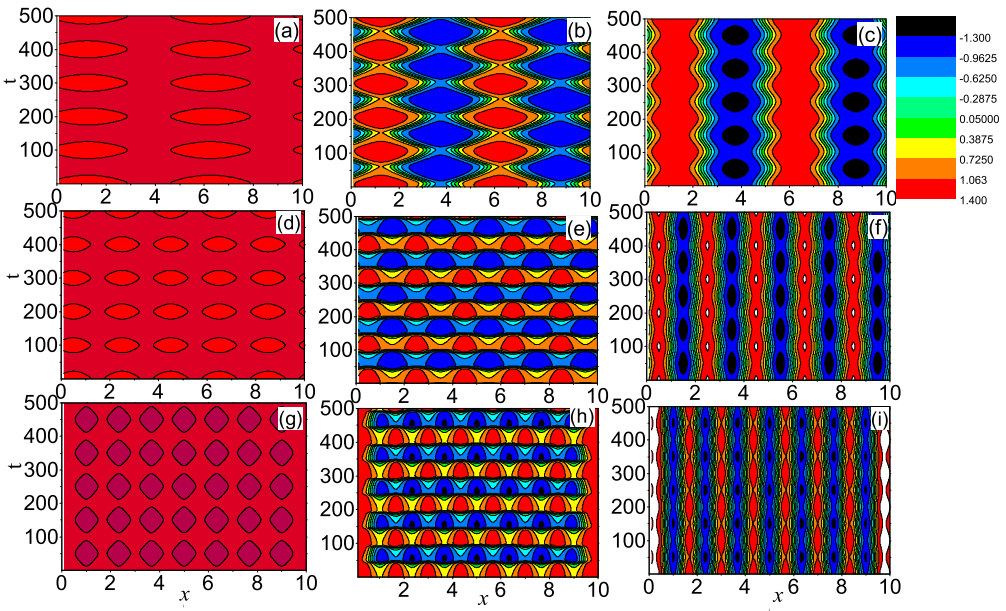

FIG. 5. (Color online) Spatiotemporal evolution of $X(x,t)$ for different values of f and c. From the top row to the bottom row, different f are chosen: $f = 2.0$, 5.0, and 7.5, respectively. From the left-hand column to the right-hand column, different c are chosen: $c < c^*$, $c = c^*$, and $c > c^*$, respectively. Specifically, $c = 0.15$ (a), 0.3 (b), 1.0 (c), 0.15 (d), 0.8 (e), 2.0 (f), 0.15 (g), 1.3 (h), and 2.0 (i).

initial conditions. We discard the transient at the beginning of the evolution. For the rows, from top to bottom, $f = 2$, 5, and 7.5. For the columns, from left to right, different values of c are chosen: $c < c^*$,$c = c^*$, and $c > c^*$ (c^* is the peak position). Comparing any three subfigures in each row, we do find the dynamical change from bistable to monostable, and the oscillation mode jumping from temporal to spatial oscillation. The left column in Fig. 5 gives examples of the evolution $X(x,t)$ with the small spatial force. The regular spatiotemporal patterns are observed, and $X(x,t)$ becomes fluctuating about 1.0 with small amplitude, signifying that the system is bistable, whereas for $c \geqslant c^*$ in the right column, the system is in monostable state. For different spatial frequencies f, we also find the strong modulation effect by spatial force with an increase of c. $X(x,t)$ oscillates with large amplitude in the spatial direction and with small amplitude in the temporal direction for sufficiently large c. However, the middle column in Fig. 5 shows that $X(x,t)$ oscillates with large amplitude in the temporal direction and with small amplitude in the spatial direction at middle c.

IV. SPATIAL-SYNCHRONIZATION-ENHANCED RESONANCE

From Fig. 1(c), a clear resonant curve can be drawn for the local maxima Q_t on the (c, f), plane and its peak values depend on the values of both f and c. The local maxima of temporal resonance factor Q_t against spatial frequency f is shown in Fig. 6. The local maxima Q_t nonmonotonously depend on the spatial frequency f. Interestingly, those large Q_t are located at $f = n$ for $n = 4$, 5, 6, 7, 8, 9, and 10, indicating that the system response gets stronger at proper values of both f and c (usually f are integers). The maximal Q_t is located at $n = 5$. Clearly, Fig. 6 shows a novel behavior of the spatially periodic-force-induced resonance largely enhanced by the spatial frequency at $f = n$.

So far we know that the spatially periodic-force-induced resonance can occur for large enough f, as shown in Fig. 1. However, it remains unclear how the spatially periodic-force-induced resonance can be enhanced by the proper frequency of spatial force. Toward that end, we check $Z(x) = \frac{1}{T}\int_{T_0}^{T_0+T} X(x,t)dt$, $X(x,t_1)$, and $X(x,t_2)$ [in which t_1 and t_2 are the times of the local maximal and minimal values of $Y(t)$, respectively] for the parameter set (f, c^*) as the same as the middle column in Fig. 5. Comparing three subfigures in Fig. 7, $X(x,t_1)$, $X(x,t_2)$, and $Z(x)$ vary periodically with spatial frequency f if $f = n$ [Figs. 7(a) and 7(b)]. Although the system does not oscillate periodically in the whole region $0 \leqslant x \leqslant L$, the periodic oscillation can be observed in the partial region of $L_{c1} \leqslant x \leqslant L_{c2}$ when f is not an integer [Fig. 7(c)]. To quantify the degree of the system entrained by the spatial force, we define the ratio R for the length of interval where $X(x,t_1)$, $X(x,t_2)$, and $Z(x)$ oscillate periodically, which is given by

$$R = \frac{L_{c2} - L_{c1}}{L}. \tag{4}$$

Obviously, $R = 1$ if the system is entrained completely by the spatial force, and $R = 0$ means that the spatially periodic-force-induced resonance does not occur at all in the system. We also calculate the amplitude A of the mean field, which is defined as the difference between the maximum and minimum of $Y(t) = \frac{1}{L}\int_0^L X(x,t)dx$ since the temporal resonance factor Q_t characterizes the signal output of the mean field $Y(t) = \frac{1}{L}\int_0^L X(x,t)dx$. The changes for R and A as a function of f are shown in Fig. 8. Comparing Fig. 8(a) with Fig. 6, we find that Q_t nonmonotonously depends on the spatial frequency f due to the change of the system's amplitude A. However, temporal resonance factor Q_t becomes much larger at some spatial frequencies ($f = n$) because the

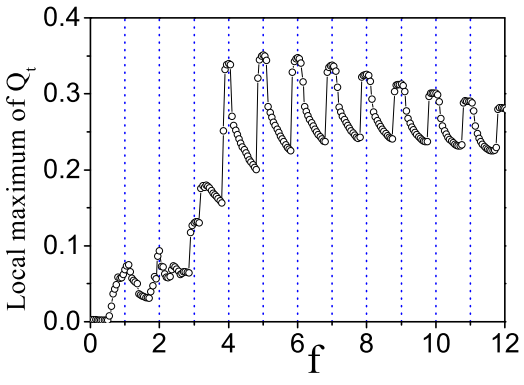

FIG. 6. (Color online) The local maximum Q_t against f, showing the enhanced spatially periodic-force-induced resonance at certain special frequencies.

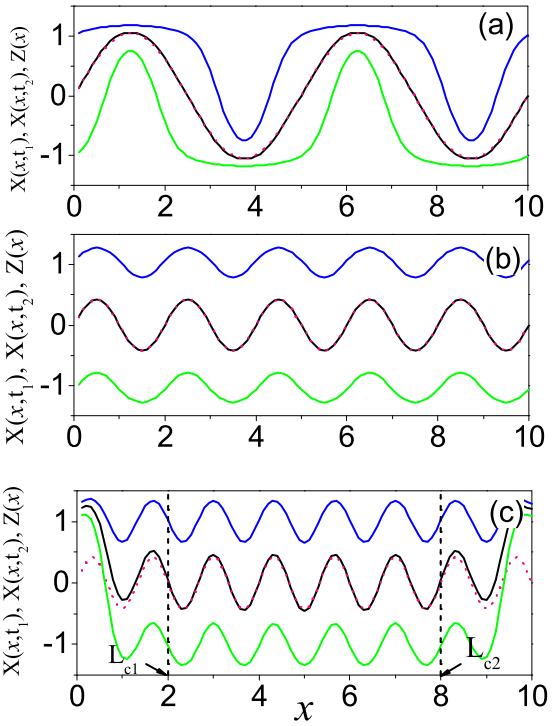

FIG. 7. (Color online) (a)–(c) The spatial series of $X(x,t_1)$ $X(x,t_2)$ and $Z(x) = \frac{1}{T}\int_{T_0}^{T_0+T} X(x,t)dt$ for $f = 2.0$,5.0, and 7.5, respectively. t_1 and t_2 are the time of the local maximal and minimal value of $Y(t)$, respectively. From top to bottom, the blue, black, and green lines correspond to $X(x,t_1)$, $Z(x) = \frac{1}{T}\int_{T_0}^{T_0+T} X(x,t)dt$, and $X(x,t_2)$, respectively. The pink dots stand for $A(f)\sin(2\pi f\frac{x}{L})$.

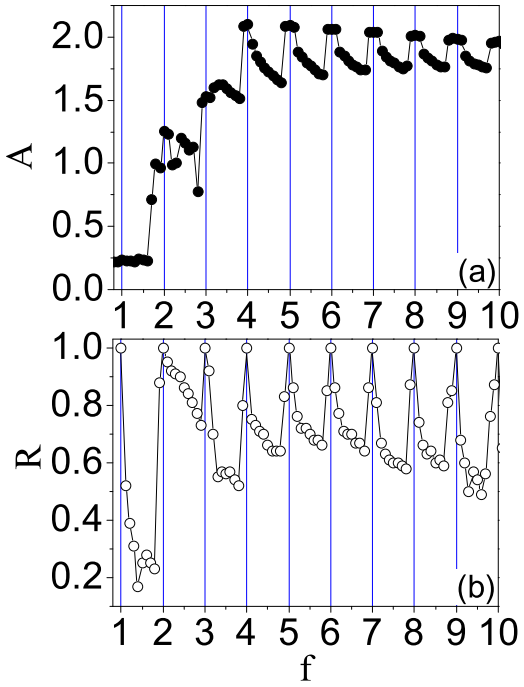

FIG. 8. (Color online) The amplitude A of mean field $Y(t) = \frac{1}{L}\int_0^L X(x,t)dx$ (a) and the ratio R ($R = \frac{L_{c2}-L_{c1}}{L}$) (b) against frequency f.

system synchronizes with spatial force, which is given by $R = 1$ at $f = n$ in Fig. 8(b). Here we call the behavior of large Q_t at $R = 1$ *the spatial-synchronization-enhanced resonance*. Since the dynamics of the system should be influenced by both the amplitude and frequency of the spatial force, it is easy to understand the occurrences of the spatially periodic-force-induced resonance and the spatial-synchronization-enhanced resonance shown in Fig. 6.

V. CONCLUSION

In conclusion, we have studied the spatially periodic-force-induced resonance in the reaction-diffusion system so that the response of the system to the weak signal can be optimized by the spatial force with intermediate amplitude and sufficiently large spacial frequency. We also observed that the resonance can get stronger when the reaction-diffusion system is synchronizing with the spatial force at a certain frequency. Thus, the maximal response of the reaction-diffusion system to the weak signal can be achieved when both the spatially periodic-force-induced resonance and spatial-synchronization-enhanced resonance occur at a certain spatially periodic force. We suggest that the spatially periodic-force-induced resonance observed in the reaction-diffusion system with spatial force and a weak signal may play a significant role in engineering and natural systems.

ACKNOWLEDGMENTS

This work was supported partially by the National Natural Science Foundation of China under Grants No. 11205103, No. 11275129 (C.G.Y.), and No. 31370830 (J.W.S.), the National Science Foundation for Post-doctoral Scientists of China under Grants No. 0660-K83003 (C.G.Y.), China National Funds for Distinguished Young Scholars under Grant No. 11125419, and the Fujian Province Funds for Leading Scientist in Universities (J.W.S.).

[1] K. Wiesenfeld and F. Moss, Nature (London) **373**, 33 (1995).
[2] P. Jung and P. Hänggi, Phys. Rev. A **44**, 8032 (1991).
[3] G. Hu, H. Haken, and C. Z. Ning, Phys. Rev. E **47**, 2321 (1993).
[4] B. McNamara, K. Wiesenfeld, and R. Roy, Phys. Rev. Lett. **60**, 2626 (1988).
[5] L. Gammaitoni, F. Marchesoni, E. Menichella-Saetta, and S. Santucci, Phys. Rev. Lett. **62**, 349 (1989).
[6] V. S. Anishchenko, M. A. Safonova, and L. O. Chua, Int. J. Bifurcation Chaos **4**, 441 (1994).
[7] D. S. Leonard and L. E. Reichl, Phys. Rev. E **49**, 1734 (1994).
[8] S. M. Bezrukov and I. Voydanoy, Nature (London) **378**, 362 (1995).
[9] R. Benzi, G. Parisi, A. Sutera, and A. Vulpiani, Tellus **34**, 10 (1982).
[10] J. W. Shuai and P. Jung, Phys. Rev. Lett. **95**, 114501 (2005).
[11] J. W. Shuai and P. Jung, Proc. Natl. Acad. Sci. (USA) **100**, 506 (2003).
[12] I. I. Blekhman and P. S. Landa, Int. J. Non-Linear Mech. **39**, 421 (2004).
[13] C. J. Tessone, C. R. Mirasso, R. Toral, and J. D. Gunton, Phys. Rev. Lett. **97**, 194101 (2006).
[14] R. Toral, C. J. Tessone, and J. V. Lopes, Eur. Phys. J. Spec. Top. **143**, 59 (2007).
[15] C. J. Tessone, Ph.D. thesis, Universitat De Les Illes Balears Departament De Física, 2006.
[16] M. Gassel, E. Glatt, and F. Kaiser, Phys. Rev. E **76**, 016203 (2007).
[17] E. Glatt, M. Gassel, and F. Kaiser, Phys. Rev. E **75**, 026206 (2007).
[18] H. S. Chen, J. Q. Zhang, and J. Q. Liu, Phys. Rev. E **75**, 041910 (2007).
[19] E. Ullner, A. Zaikin, J. Garcia-Ojalvo, R. Bascones, and J. Kurths, Phys. Lett. A **312**, 348 (2003).
[20] C. Stan, C. P. Cristescu, D. Alexandroaei, and M. Agop, Chaos Solitons Fractals **41**, 727 (2009).
[21] D. Cubero, J. P. Baltanás, and J. Casado-Pascual, Phys. Rev. E **73**, 061102 (2006).
[22] X. X. Wu, C. G. Yao, and J. W. Shuai, Sci. Rep. **5**, 7684 (2015).
[23] J. Casado-Pascual and J. P. Baltanás, Phys. Rev. E **69**, 046108 (2004).
[24] V. N. Chizhevsky and G. Giacomelli, Phys. Rev. E **73**, 022103 (2006).
[25] V. N. Chizhevsky and G. Giacomelli, Phys. Rev. E **70**, 062101 (2004).

[26] V. N. Chizhevsky and G. Giacomelli, Phys. Rev. A **71**, 011801 (2005).
[27] A. A. Zaikin, L. López, J. P. Baltanás, J. Kurths, and M. A. F. Sanjuán, Phys. Rev. E **66**, 011106 (2002).
[28] V. M. Gandhimathi, S. Rajasekar, and J. Kurths, Phys. Lett. A **360**, 279 (2006).
[29] C. G. Yao and M. Zhan, Phys. Rev. E **81**, 061129 (2010).
[30] C. G. Yao, Y. Liu, and M. Zhan, Phys. Rev. E **83**, 061122 (2011).
[31] J. P. Baltanas, L. Lopez, I. I. Blechman, P. S. Landa, A. Zaikin, J. Kurths, and M. A. F. Sanjuan, Phys. Rev. E **67**, 066119 (2003).
[32] K. M. Page, P. K. Mainib, and N. A. M. Monkc, Physica D **202**, 95 (2005).
[33] M. Dolnik, I. Berenstein, A. M. Zhabotinsky, and I. R. Epstein, Phys. Rev. Lett. **87**, 238301 (2001).
[34] R. Manor, A. Hagberg, and E. Meron, New J. Phys. **11**, 063016 (2009).